

# OPTIMAL PLACEMENT OF AN AIRFLOW PROBE AT A MULTIROTOR UAV FOR AIRBORNE WIND MEASUREMENTS

C. Molter<sup>1</sup>, P. W. Cheng<sup>1</sup>

<sup>1</sup>University of Stuttgart, Wind Energy Research Group (SWE),  
Allmandring 5B, 70569 Stuttgart, Germany, molter@ifb.uni-stuttgart.de

## Abstract

For airborne wind measurements at the Wind Energy Research Group at the University of Stuttgart it is planned to use a group of nine multirotor systems to measure environmental quantities. During the design phase of the multirotor system concerns regarding the influence of the aircraft's rotors on flow measurements have to be addressed. Also the propeller wake of one aircraft may have a great effect on the other aircraft in the group. To deal with this concerns a parameter study has been conducted using a simple two dimensional CFD simulation with an actuator disc model. To verify the simple model a more sophisticated three dimensional simulation with a rotating rotor has been performed for the most relevant operating point of the multirotor. Eventually wind tunnel experiments have been designed to measure the influence in front of the rotors and the wake direction.

While the two different models showed reasonable agreement for the investigation of the influence in front of the rotor some differences in the exact development of the wake exist. Nevertheless the extension of the rotor wake could be estimated sufficiently for the planned field measurement campaign and further improvements to the wake estimation have been suggested.

## 1. INTRODUCTION

### 1.1. Planned Measurement Aircraft

In the scope of research project ANWIND (applied wind field research) the Stuttgart Wind Energy Research Group (SWE) at the Institute of Aircraft Design at the University of Stuttgart is planning to perform unmanned airborne atmospheric measurements near wind turbines with a group of nine rotary wing aircraft. These aircraft will be designed in a multirotor configuration with MTOW below 5kg to avoid further legal limitations.

Airborne atmospheric measurements have already been performed in the sector of wind energy and boundary layer research with fixed wing aircraft and larger rotary wing aircraft during the past years ([1],[2]). The idea of using a group of small rotary wing aircraft to hover at discrete points in space simultaneously is however relatively new.

The planned measurement multicopter, called ANDroMeDA – ANWIND Drone for measurement and Data Acquisition – will be equipped with temperature and pressure sensors as well as a flow measurement probe. The used probe can be either a simple pitot tube, multihole pitot tube or a hot wire probe.

One of the main concerns during the preliminary design of this aircraft was the effect of the rotor

induced airflow on the wind measurement. An effect of the rotor flow on the measurement probe is suspected to greatly reduce the measurement accuracy. Also the rotor wake of one aircraft in the formation is suspected to have a significant influence on the measurement process of other group members if they are hovering behind.

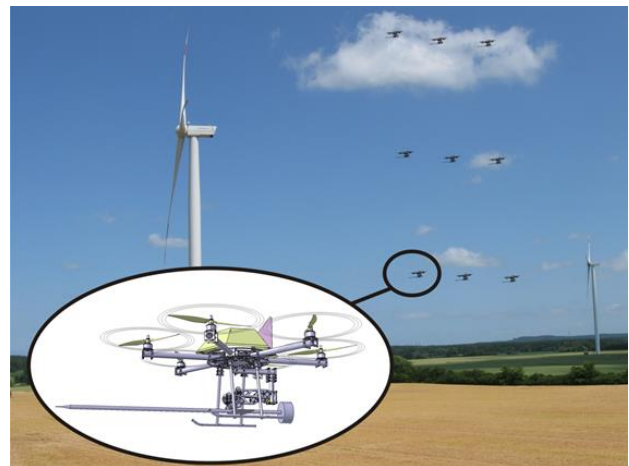


Figure 1: Planned measurement with a group of nine aircraft

### 1.2. Analytical Approaches to model the Rotor Wake

The maximum induced velocity in the rotor wake and the wake direction close to the rotor can be

addresses by two relatively simple, analytical approaches. The maximum induced velocity in the wake can be derived by momentum theory. For the aircraft propeller or helicopter rotor in climb the thrust is related to the induced velocity by [3]:

$$(1) \quad T = 2\rho A(v_{\infty} + v_i)v_i$$

For the inclined rotor the thrust calculates to [3]:

$$(2) \quad T = 2\rho A \cdot v_{res} \cdot v_i \\ = 2\rho A \cdot \sqrt{(v_{\infty} \cdot \cos(\alpha) + v_i)^2 + (v_{\infty} \cdot \sin(\alpha))^2} \cdot v_i$$

For both cases these equations do not express how far behind the rotor disc the maximum induced velocity is reached. In the classic momentum theory it is often spoken of “far away from the disc”.

The direction of the rotor wake can also be calculated analytically with a simplified approach if the vectors of the induced velocity and inflow velocity are added (fig. 2)

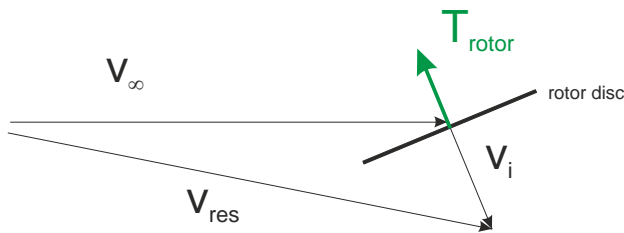


Figure 2: Simplified approach to calculated resulting velocity in the rotor wake [3].

But without any knowledge about the development of the induced velocity over distance a prediction of the rotor wake direction is not possible.

No analytical approaches can be found on the flow in front of the rotor disc.

### 1.3. Proposed Approach

The proposed approach to overcome these uncertainties includes two-dimensional CFD simulations with an actuator disc model. These simulations need very little computation time and many different cases can be investigated. To quantify the error introduced by the actuator disc method compared to a rotating rotor a three-dimensional simulation with a moving grid is additionally performed for the most relevant operating case of ANDroMeDA. Eventually wind tunnel tests are conducted to validate the simulations wherever possible.

## 2. FLIGHT CONDITIONS OF THE MEASUREMENT AIRCRAFT

To make sure that all investigations will match the range of operating conditions of the developed aircraft the possible inflow speeds, inclination angles of the rotor and disc loadings have to be determined.

Because AnDroMeDA will be hovering at a fixed location over ground the wind speed to measure will also be the rotor inflow velocity. Since wind measurements below  $v_{\infty}=4\text{m/s}$  are not useful in the field of wind energy and the nominal wind speed of the most wind turbines lies between  $10\text{m/s}$  and  $12\text{m/s}$  a range between  $v_{\infty}=4\text{m/s}$  and  $v_{\infty}=12\text{m/s}$  was selected for the simulations and wind tunnel tests.

The disc loading of the AnDroMeDA rotors was not defined when the investigations started. The range was selected empirically considering existing multirotor aircraft shown in tab. 1.

Copter Name	No of rotors	TOW [g]	$D_{rotor}$ [m]	D.L. [N/m <sup>2</sup> ]
JXD Airbus	4	12.2	0.03	42
Hubsan X4	4	35	0.055	36
3D Robotics DIY Kit	4	1900	0.254	92
SWE Hexacopter	6	4000	0.3302	76

Table 1: Disc Loading for different multicopter models.

Since a wide range should be investigated the disc loading range was defined to  $D.L. = 20\text{ N/m}^2 \dots 125\text{ N/m}^2$

The rotor inclination angle, hence angle of attack of the aircraft, depends on the ratio of aircraft weight to aircraft drag (see fig. 3 and eq. 3).

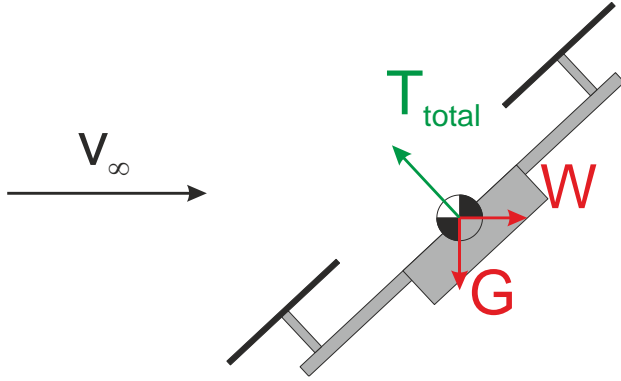


Figure 3: Estimation of the inclination angle.

$$(3) \quad D = c_D \frac{\rho}{2} v_{\infty}^2 A \longrightarrow v_{\infty}(\theta) = \sqrt{\frac{2 \cdot G \cdot \tan(\theta)}{c_D \cdot \rho \cdot A}}$$

The aircraft drag was estimated according to inflight measurements (Angle of Attack over Airspeed) from the existing SWE hexacopter. Since AnDroMeDA is planned to be much slimmer than the SWE hexacopter this is a quite conservative estimation.

The range of rotor inclination angles determined by these estimations is  $\alpha_{disc} = 5^\circ \dots 45^\circ$ .

### 3. SIMULATION SETUP

For all simulations ANSYS CFX was used. The actuator disc was realized by a subdomain with a volume based momentum source term, called “general momentum source” in CFX. The thrust of the disc calculates to:

$$(4) \quad T = \text{General Momentum Source Term} \cdot D \cdot t \cdot h$$

Where D is the rotor diameter, t is the thickness of the disc and h is the disc width. To achieve numerical stability the value for the source term was slowly increased to its nominal value during the first 10 iterations.

Because the momentum source can be given as a function of grid coordinates it is also possible to model thrust distribution over rotor radius. But since no explicit propeller model has been chosen for the multicopter system yet the lift distribution has not been modeled in 2D simulations at the present state.

Modeling turbulence in CFD simulations generally has to be done carefully. When specifying a turbulence intensity at the inlet boundary surface the turbulence intensity in the control volume quickly decreases over distance due to dissipation. To

investigate the rotor wake decay the effect of ambient turbulence was also of interest.

To model the ambient turbulence an artificial turbulence source term was added as described in [4]. In ANSYS CFX a scalar quantity with the unit of  $W/m^3$  can be set up as a source term for turbulent kinetic energy (TKE).

Because no absolute value for the TKE or the turbulence intensity (T.I.) can be set with this method the actual local TKE in the control volume during simulation time is used at each timestep to calculate the source term:

$$(5) \quad TKE_{source} = p \cdot (TKE_{desired} - TKE_{actual})$$

The desired TKE can be determined by the desired ambient turbulence intensity:

$$(6) \quad TKE_{desired} = \frac{3}{2} \cdot (T.I._{desired} \cdot u)^2$$

Unfortunately this does yield in a constant T.I. and the parameter p has to be adjusted for each simulation case.

The physical meaning of this source term has to be considered very carefully. All simulations were also run without any artificial turbulence to be able to study its effects and to be able to compare. A more complex modeling of ambient turbulence is beyond the scope of this project and can only be validated with intensive field testing since we want to model varying environmental conditions. The length scales and spectra are for example expected to change greatly from flat terrain to complex terrain.

All meshes for the quasi 2D simulations are structured hexahedral meshes with only one element in the third dimension. For all meshes the thickness of the actuator disc is 0.1D. The disc consists of 60 elements in diameter and 15 elements in thickness (see fig. 5)

Fig. 4 illustrates the mesh for straight propeller inflow. The Mesh consists of 94 829 elements.

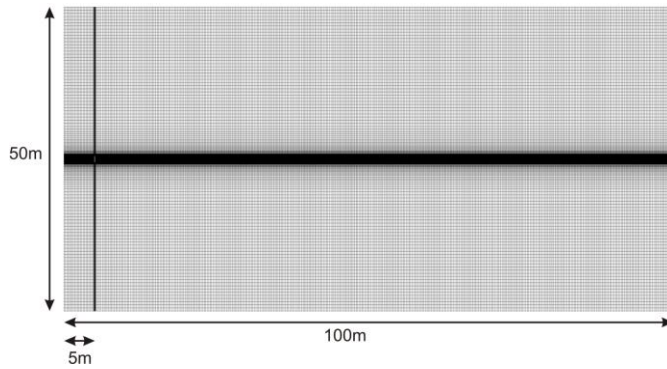


Figure 4: Mesh for straight inflow (propeller) cases.

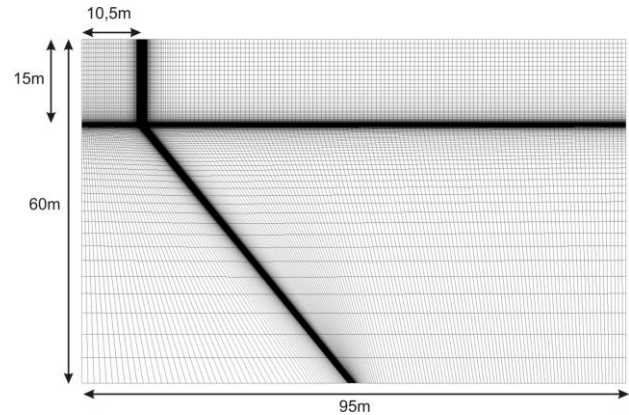


Figure 6: Mesh for a rotor at angle of attack at  $\alpha_{disc} = 45^\circ$ .

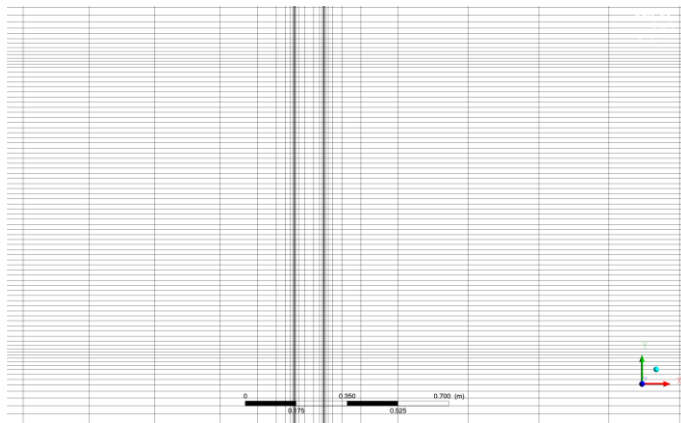


Figure 5: Refinements in the vicinity of the actuator disc.

Fig. 6 depicts a mesh for an inclined rotor. The disc is always oriented horizontally while the inflow direction is set according to the inclination angle. Two different meshes were created to place the refinements as close as possible to the rotor wake direction for the entire range of inclination angles. The meshes both consist of 46 096 elements. As a result of the topology at the lower left corner some non-orthogonal, highly skewed elements exist. However the flow in this region is considered not to be relevant to the problem.

To make sure the meshes are not too coarse some simulations were also performed with 214 839 elements for the straight inflow and 105 820 elements for the inclined inflow. When using a source term to model the ambient turbulence as previously described no significant differences could be revealed and therefore the meshes shown above were used. Without modeling ambient turbulence non-negligible differences in the wake occurred. These differences only applied to the far wake and not to the flow region in front of the rotor or the wake direction. Knowing that predicting the wake decay without any influence of ambient turbulence will be not possible even with a finer mesh this effect was neglected.

For the three-dimensional simulations a rotating three-bladed propeller of type Master Airscrew 13x6 (13 inch diameter) was modeled. The unstructured tetrahedron mesh consists of 5.95 million elements. As seen in fig. 7 and fig. 8 the rotor blades are modeled relatively fine including prism layers to resolve the boundary layer to some degree. Around the cylindrical rotating mesh another cylindrical area is defined as mesh refinement area. The entire area where the wake is expected was refined to some extent (see fig. 9).

Mesh Name	Dedicated Inflow Direction	$D_{\text{rotor}}$ [m]	No. of Elements
Mesh_ON	0°	1.0	94 829
Mesh_OF	0°	1.0	214 839
Mesh_22N	22.5°	1.0	46 096
Mesh_22F	22.5°	1.0	105 820
Mesh_45N	45°	1.0	46 096
Mesh_45F	45°	1.0	105 820

Mesh_ON_025	0°	0.25	94 829
Mesh_ON_05	0°	0.5	94 829
Mesh_22N_025	22.5°	0.25	46 096
Mesh_22N_05	22.5°	0.5	46 096
Mesh_45N_025	45°	0.25	46 096
Mesh_45N_05	45°	0.5	46 096

Table 2: Mesh overview for 2D simulations.

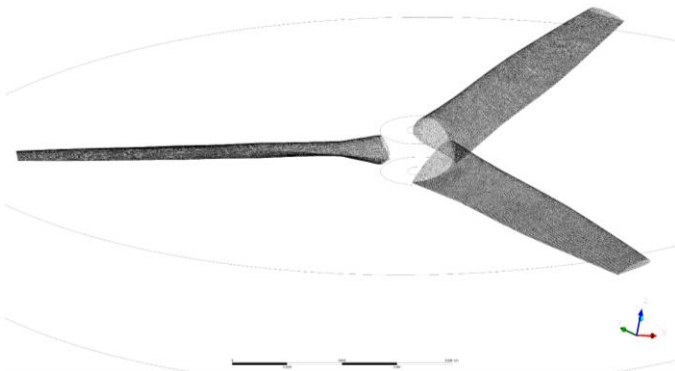


Figure 7: Mesh for the rotating rotor simulation.

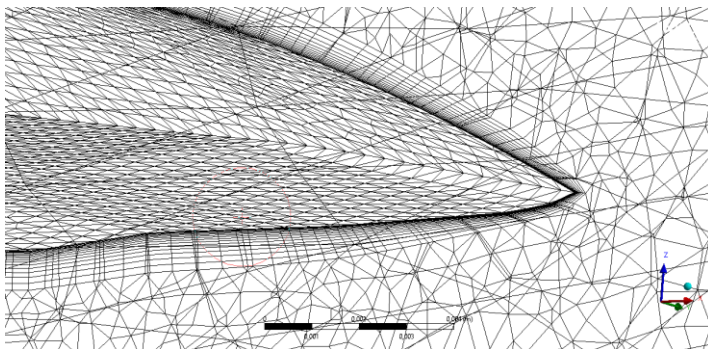


Figure 8: Prism Layers at the rotor blade.

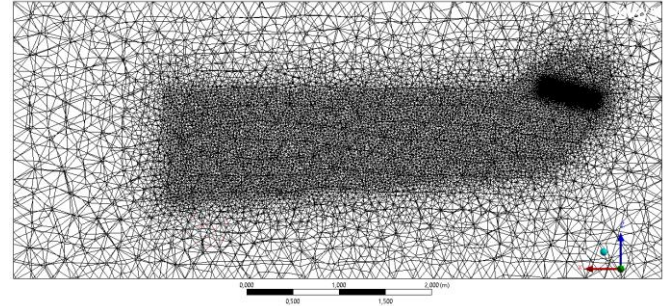


Figure 9: Refinement areas for the three-dimensional mesh.

#### 4. WIND TUNNEL SETUP

The experiments described were conducted in the medium size low speed wind tunnel at the Institute Aerodynamics and Gas Dynamics (IAG) at the University of Stuttgart. This wind tunnel is a closed Göttinger type tunnel with an open jet test section. The nozzle used has a diameter of 1.0 m.

In the middle of test section a small whirltower was mounted (fig. 10). This whirltower was able to measure RPM, thrust and torque of tested propeller as well as electrical power of the used motor. These quantities were also used in an ongoing propeller measurement campaign. For the content presented here the only important quantity measured by the whirltower is the propeller thrust. The correct thrust had to be adjusted to make sure the disc loading is comparable to the simulations.

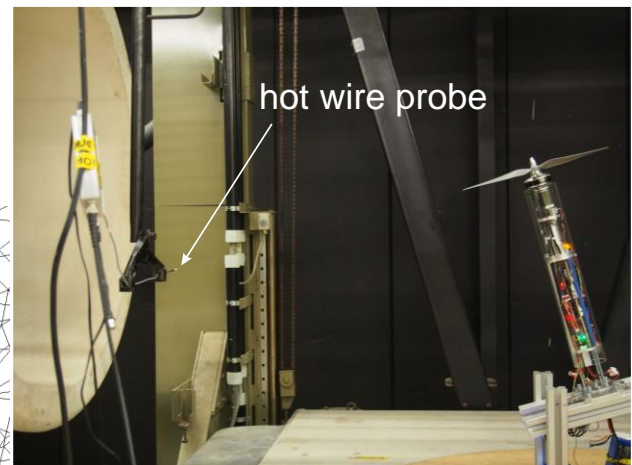


Figure 10: Whirltower mounted in the wind tunnel test section

To validate the simulations regarding wake redirection a laser sheet visualization technique was used. To measure the influence of the running propeller on the free stream velocity an one-dimensional hot wire probe was used. The used wire has a diameter of  $d_{\text{wire}}=10\mu\text{m}$  and a length of  $l_{\text{wire}}=4\text{mm}$ . It is used at a constant temperature (CTA). All measurements were sampled with 10 000 samples/s. The CTA electronic module internally uses a 5kHz low pass filter. With the help of an electric traverse system the probe could be placed at several points. Fig. 11 gives an overview of the measurement points.

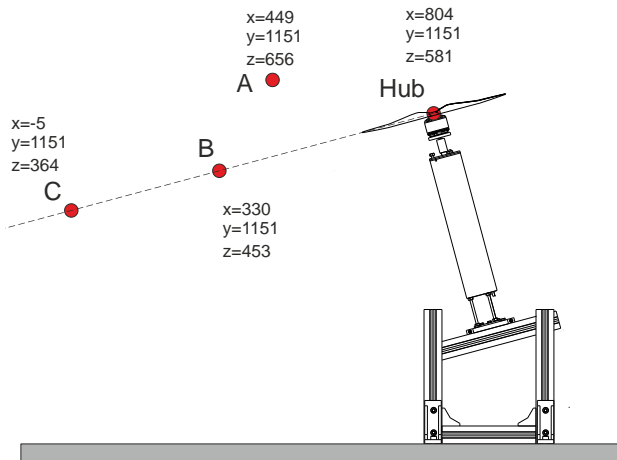


Figure 11: Hot wire measurement points in the wind tunnel. The drawing is true to scale.

## 5. INVISCID STRAIGHT INFLOW SIMULATION

According to simple momentum theory the induced velocity in the rotor wake has to be twice the induced velocity in the rotor disc:  $w = 2 v_i$ . To ensure the continuity of mass the rotor wake also has to contract to half of the rotor disc area. This assumption is only valid for ideally inviscid flow and as mentioned before it does not include any statement about the distance that is needed for the wake to fully contract.

To verify the actuator disc implementation an inviscid preliminary simulation has been carried out (fig. 12). It can be clearly seen that the wake contraction is completed in less than two rotor diameters. It can also be seen that there are no further changes in the wake since the decay of the rotor wake is a purely viscous process.

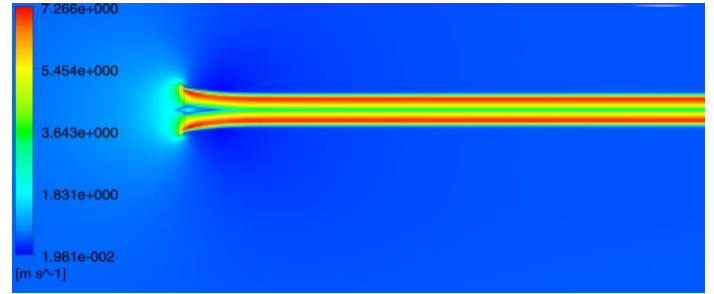


Figure 12: Inviscid actuator disc simulation.

## 6. DIMENSIONAL ANALYSIS OF THE PROBLEM

### 6.1. Straight inflow

The straight inflow propeller case was used to gain some basic understanding of the process itself. Fig. 13 shows the wake velocity of straight inflow propellers with three different diameters. The disc loading has kept constant and the distance to the disc is normalized by  $x/D$ . It can be seen that the velocity decay rate  $dv/dx$  matches very well up to  $x/D=30$ .

For larger values than  $x/D=30$  the cases start to differ. This is assumed to be originated in the mesh scaling. The control volume size and number of cells have been kept constant while the diameters have been scaled so that the dimensionless cell size in flow direction  $\Delta x/D$  at a certain position  $x/D$  is not the same for all cases. Because mixing of the propeller wake with the environment is a very sensitive process the mesh size is supposed to influence the wake decay.

To confirm this assumption further simulations have to be done with a completely scaled mesh. Since the wake decay of a straight inflow propeller is not relevant for the development of AnDroMeDA further simulations have not been made.

### 6.2. Inclined Inflow

The Scale Invariance of the inclined rotors can be described as remarkably well if the disc loading is kept constant. Since the side wards inflow introduces a lot of energy to dissolve the rotor wake the problem is also not sensitive to mesh scaling and the process is quite stable.

If normalized by  $x/D$  recommendations about minimum distance from one aircraft to another member of the group or minimum distance from

measurement probe to rotor disc are valid for all

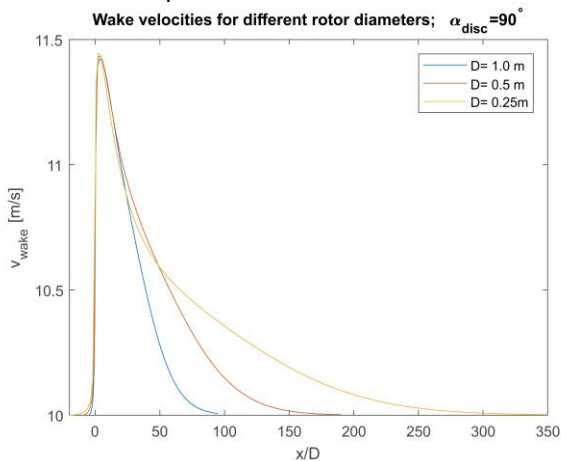


Figure 13: Wake velocities for  $D.L.=20N/m^2$  and  $v_\infty=10m/s$  at different rotor diameters.

rotor sizes at the same disc loading. Fig. 14 gives an overview of scaled rotors at an inclined angle.

## 7. INFLUENCE OF ROTOR OPERATION IN FRONT OF THE ROTOR DISC

From fig. 16 it can be seen that the actuator disc predicts a quite regular flow pattern in a shape similar to a dipole source in potential flow theory. At the top of the disc exists a region of increased velocity and at the bottom exists a symmetrical counterpart of decreased velocity. One of the main objectives running the more complex three dimensional simulation with a rotating rotor was to find out if this quite simple flow pattern will also establish here. As one can see in fig. 15 the agreement of the two simulation methods is absolutely satisfying in that region of the rotor.

The simulations predict only a minor influence on the flow measurement in front of the rotor disc by the rotor operation. To ensure the validity of the simulations hot wire measurements in the wind tunnel were conducted at a D.L. of  $75 N/m^2$  and inflow speeds of 4 m/s and 10 m/s. The propeller used was an APC 13x6.5 (13 inch diameter). The measurement locations are shown in fig.11.

Each measurement was acquired with a sampling rate of 10 000 samples/s and a duration of 10s. Because the tunnel speed is not easy to adjust and it is not easy to keep the tunnel speed absolutely constant the propeller was wether shut down or started up during the ongoing measurement. With

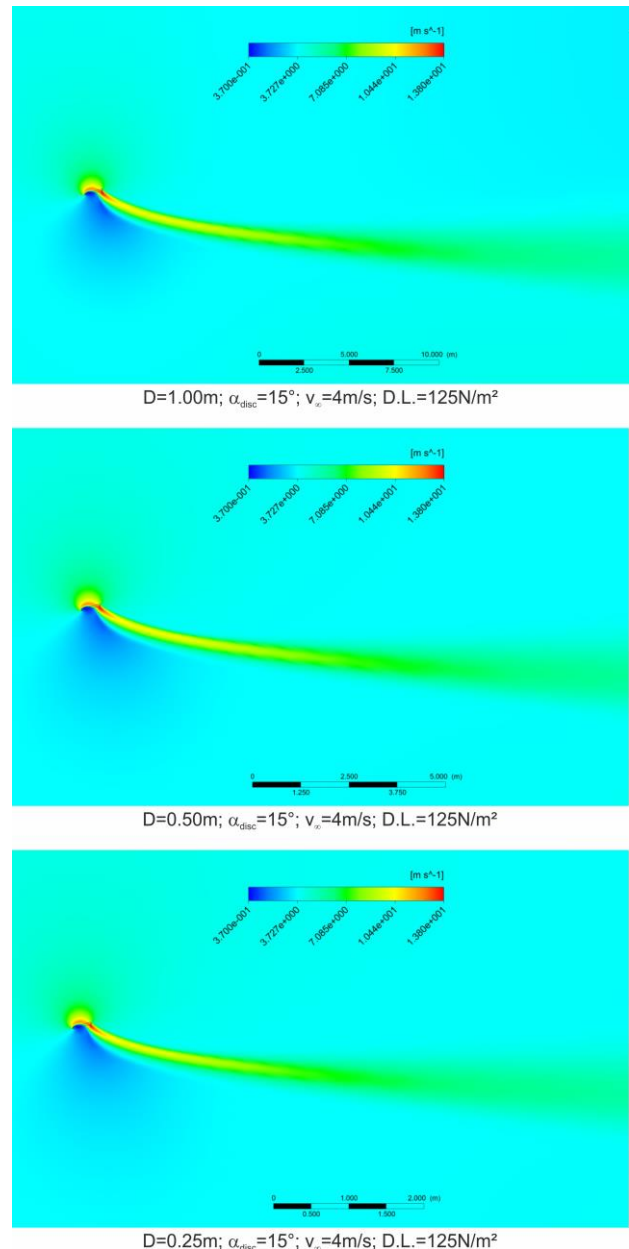


Figure 14: Rotor wake for three different rotor diameters.

this approach it is easier to distinguish between a fluctuation in tunnel speed and propeller influence. Measurements with a steady operation of the propeller were used to calculate the turbulence intensity of the inflow measurement. No change in turbulence intensity could be observed comparing measurements with and without the propeller running.

Fig. 17 shows hot wire measurements in point A and point B. While in point A the running propeller causes a higher inflow speed, in point B a running

propeller causes a lower inflow speed. This phenomena can be explained with the actuator disc simulation as shown in fig. 16.

Interestingly in some cases the rotor induced flow in point C, which is farther away from the propeller than point B, caused a slightly larger error in inflow measurement. This can also be seen in the simulations (fig. 16 and tab. 3) but to a less significant extent. One explanation could be an influence of the wind tunnel table or nozzle.

In general only a slight influence about 1% to 2% error can be recognized at the nominal operating point of  $v_\infty=10\text{m/s}$  even at point A very close to the propeller. At an operation at 4 m/s the error is larger but still acceptable for field measurements.

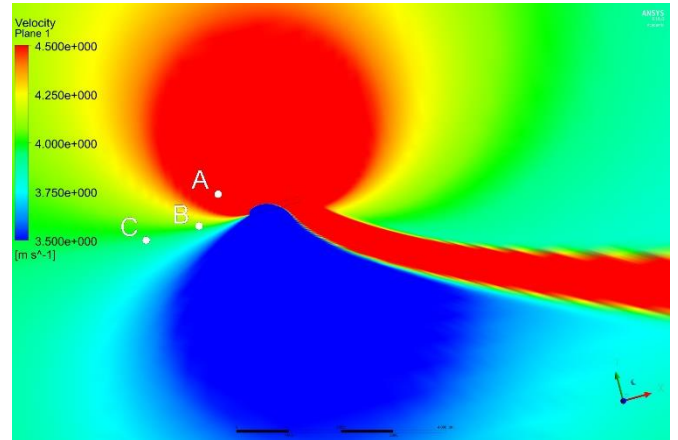


Figure 16: Hot wire measurement points in 2D simulation with extensively drawn velocity range.

	Point A	Point B	Point C
$\Delta u$ at $v_\infty = 4\text{m/s}$	+1.18	+0.028	-0.06
$\Delta u$ at $v_\infty = 10\text{m/s}$	+0.46	-0.042	-0.043

Table 3: Velocity changes predicted by the 2D simulation.

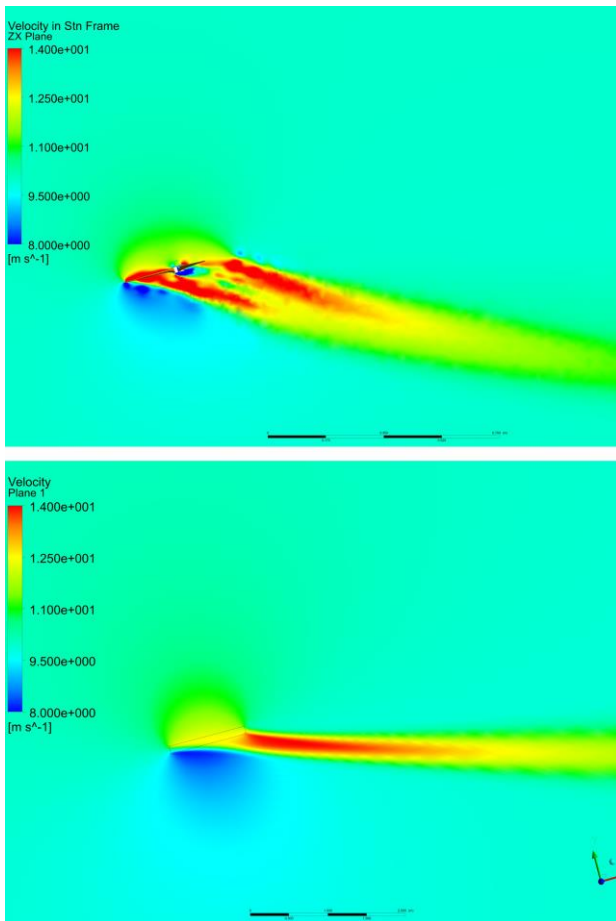


Figure 15: 2D actuator disc simulation in comparison to the 3D simulation with a rotating rotor.  $D.L.=70 \text{ N/m}^2$ ;  $v_\infty=10\text{m/s}$ ;  $\alpha_{disc} = 15^\circ$ .

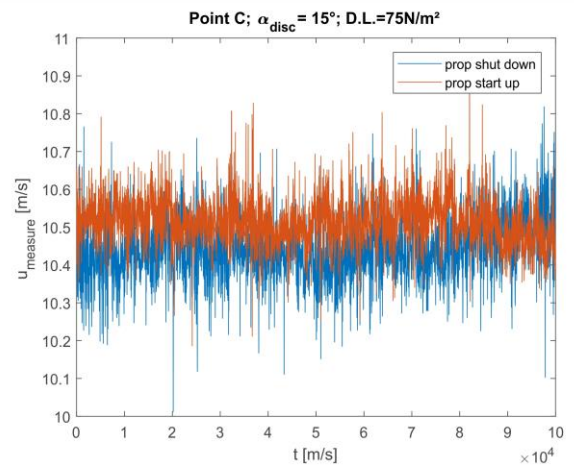
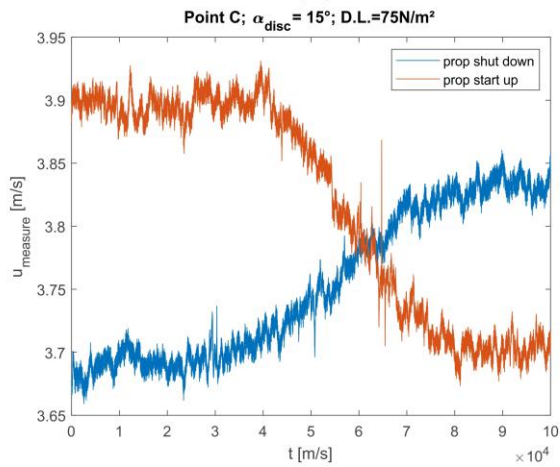
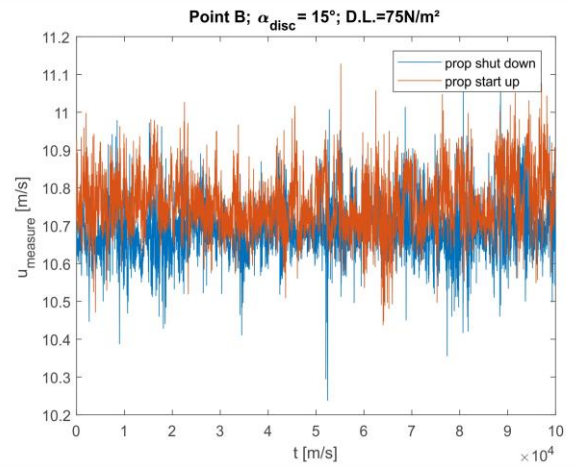
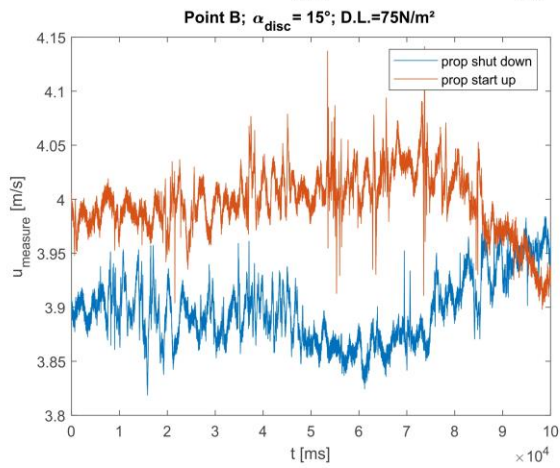
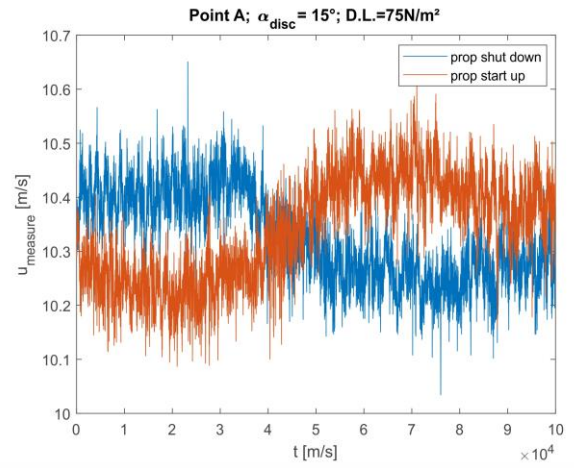
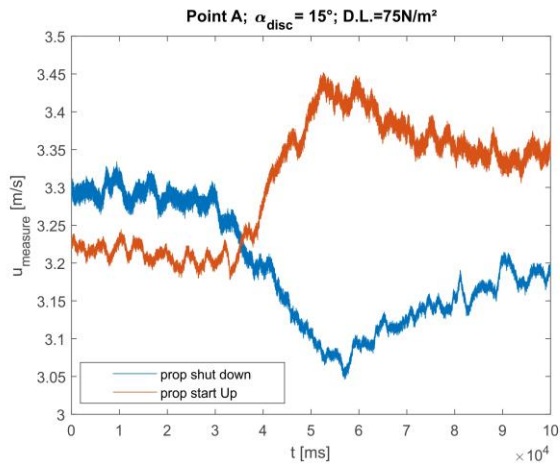


Figure 17: Hot Wire Measurements at  $v_\infty=4\text{m/s}$ .

Figure 18: Hot Wire Measurements at  $v_\infty=10\text{m/s}$ .

## 8. ROTOR WAKE DEFLECTION

Comparing the simple approach of adding the induced velocity and the inflow velocity with the 2D actuator disc simulations reveals that an acceptable agreement can only be achieved very close to the rotor. The rotor wake realigns parallel to the inflow usually within less than  $z_d < 10D$ . The amount of displacement depends on the ratio between inflow speed and  $v_i$ . Fig. 20 gives an example over a wide variety of parameters.

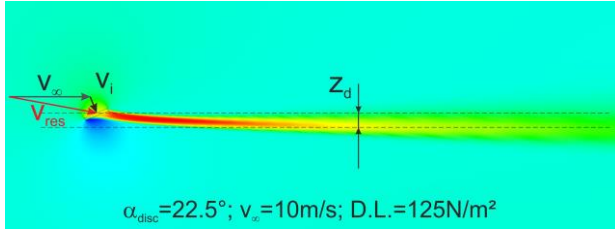


Figure 19: Realignment of the wake. The length of  $v_\infty$  and  $v_i$  arrows was scaled to truth (eq. 2)

When the most relevant operating case is compared between the 3D and 2D simulation (fig. 15) it can be clearly seen that the effect of wake redirection is underestimated by the actuator disc method. It is assumed that the constant thrust distribution over the entire disc has some influence on that issue because at a more realistic thrust distribution the induced velocity also reaches higher values at the outer halves of the rotor blades. In the future a 2D simulation with a slightly modified model, accounting for the thrust distribution along the disc radius, will be tested. Even with the rotating rotor simulation the wake is still displaced less than  $z_d = 10D$ .

The wake direction was also investigated during wind tunnel tests by a laser sheet visualization technique. Fig. 21 shows the wind tunnel test compared to the simulations. Another effect that occurred in the wind tunnel tests that was not accounted for in the simulation is the stagnation region of the whirltower itself. However this effect does also not occur for a real multirotor design which usually incorporates much thinner horizontal carbon tubes to mount the motors and propellers.

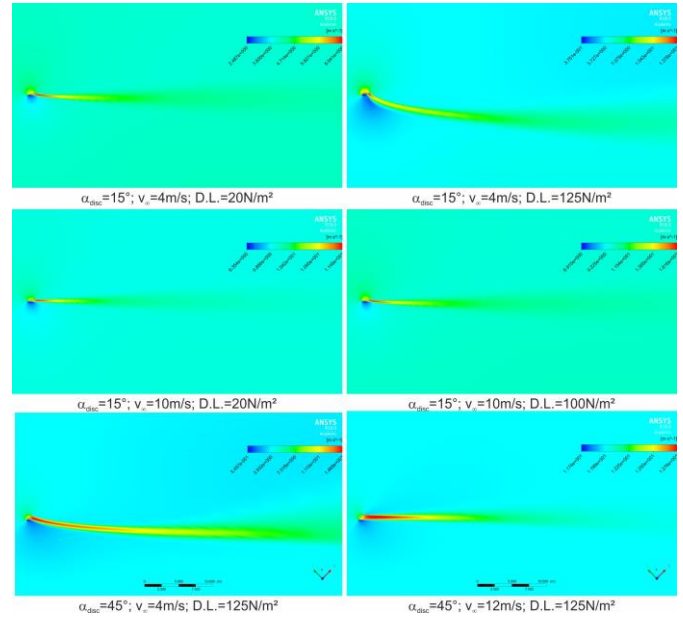


Figure 20: Overview of some simulation cases.

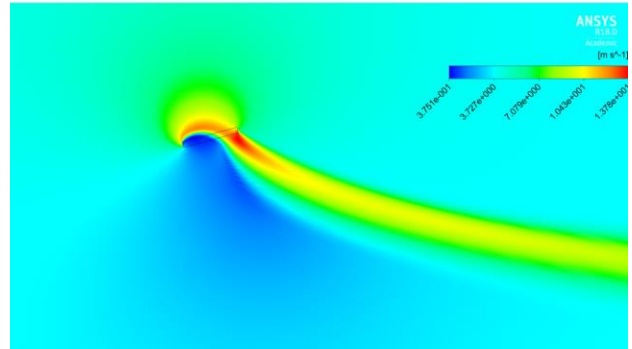
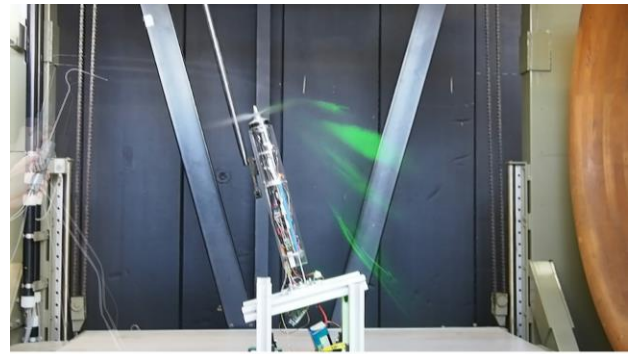


Figure 21: Comparison of wake redirection in wind tunnel experiment and simulation at  $D.L. = 125 \text{ N/m}^2$ ;  $v_\infty = 4 \text{ m/s}$ ;  $\alpha_{disc} = 15^\circ$ .

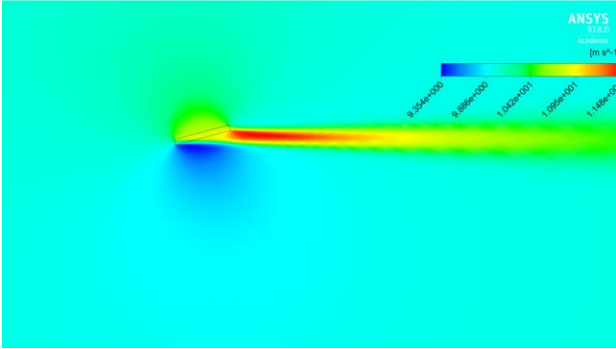
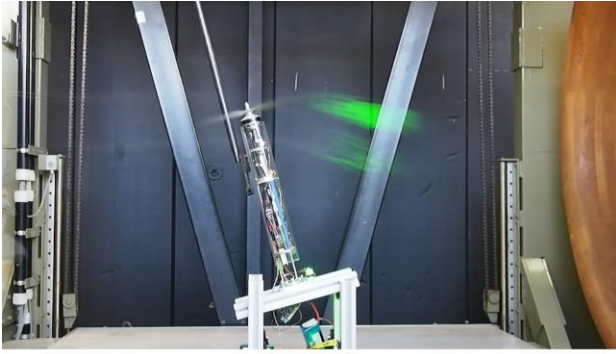


Figure 22: Comparison of wake redirection in wind tunnel experiment and simulation at  $D.L.=20 \text{ N/m}^2$ ;  $v_\infty=10\text{m/s}$ ;  $\alpha_{disc}=15^\circ$ .

## 9. ROTOR WAKE DECAY

### 9.1. Maximum Velocity in the Wake

The simulations showed that the maximum induced velocity is reached at a point very close to the rotor disc. This can be observed in fig. 24. The maximum induced velocity theoretically reached is twice the value derived in eq. 1 for straight inflow and eq. 2 for inclined inflow. This simple analytical approach shows good agreement with the simulations (fig. 23). Tab. 4 additionally offers a comparison between maximum wake speeds measured in the wind tunnel with a handheld anemometer and maximum wake speeds according to the 2D simulations. Even with this simple device a sufficient agreement could be achieved.

$v_\infty$ [m/s]	D.L. [ $\text{N/m}^2$ ]	$V_{\text{max}}$ measured	$V_{\text{max}}$ simulated
10.1	125	17.6	17.4
10.3	60	14.6	14.0
5.5	125	15.6	14.8
6.4	60	12.2	11.5

Table 4: Comparison of measured and simulated maximum velocities in the rotor wake.

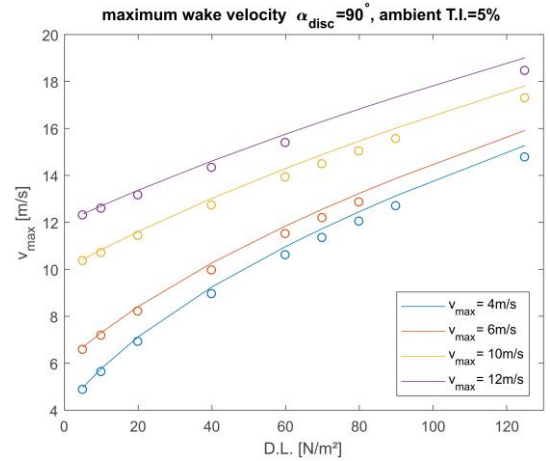


Figure 23: Maximum theoretical wake speeds compared to simulations.

### 9.2. Maximum Influence Length of the Rotor Wake

Fig. 25 compares the influence of ambient turbulence in the 2D actuator disc simulations on a straight inflow case to an inclined inflow case. It can be seen that while the ambient turbulence has a strong influence on the straight inflow case the inclined inflow case does not change so much with other turbulence levels.

If one defines the wake influence region as the region with  $(v_{\text{wake}} - v_\infty) / v_\infty > 2\%$  then fig. 24 points out that for the design case this influence length is  $< 40D$  (red horizontal line in fig. 24).

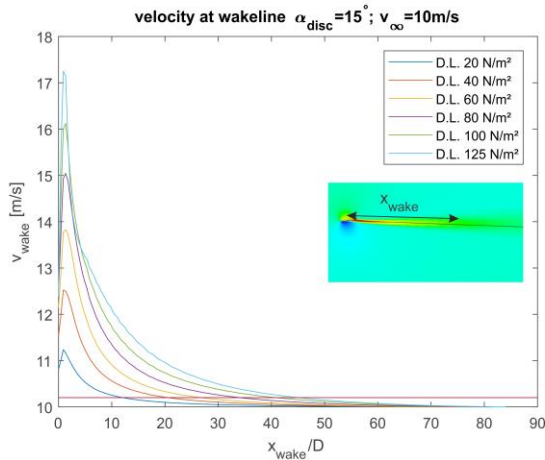


Figure 24: Decay of the rotor wake for different disc loadings.

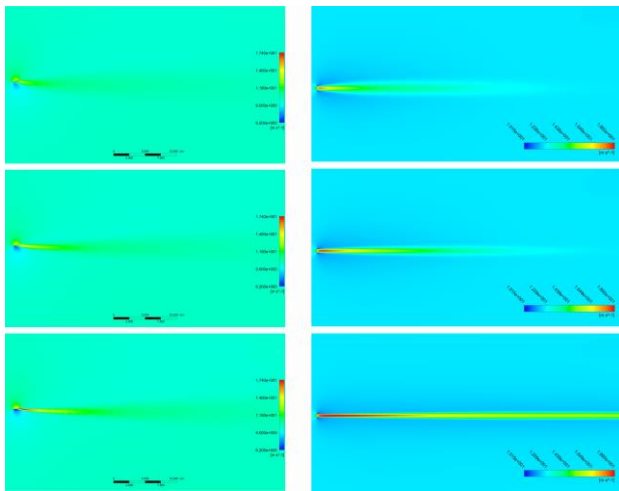


Figure 25: Effect of ambient turbulence on the wake decay rate for straight inflow and inclined inflow cases.

Fig. 26 depicts the wake decay for the three dimensional simulation with rotating rotor. The wake decays relatively soon which of course can also occur due to the coarse mesh.

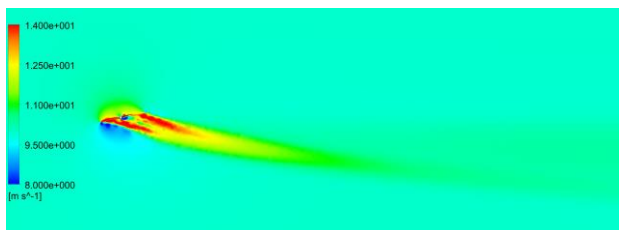


Figure 26: Wake decay in the rotating rotor simulation.

## 10. CONCLUSIONS AND OUTLOOK

The influence of rotor operation on a flow measurement probe in front of the rotor disc could be sufficiently predicted. All three methods, 2D Actuator disc simulations, 3D simulations with a rotating rotor and wind tunnel measurements, showed good agreement and therefore a clear recommendation for the probe placement can be made. According to all three methods the measurement error to expect in a distance of about two to three rotor diameters in front of the rotor hub is below 2% error for the design point of the planned airborne wind measurement aircraft, ANDroMeDA. At a lower wind speed of 4m/s the error increases to about 5% but is still acceptable for a field measurement.

Also the wake direction could be estimated to be parallel to the inflow direction and only slightly displaced perpendicular to inflow direction. The actuator disc method tends to underestimate this displacement. Nevertheless a clear recommendation can be made for planned formation flight. If two aircraft in a row are staggered by at least 10D no influence on the measurement of the rear aircraft by the rotor wake of the rotor of the front aircraft is expected.

The wake decay is difficult to predict with CFD simulations so that only field measurements can resolve this question. As the direction of the rotor wake is simply to estimate the necessary clearance for the group of wind measuring aircraft can be secured without further knowledge on the length of disturbing rotor wakes.

To improve the deficits of the simple actuator disc method an improved method, accounting for the thrust distribution along the disc, will be tested.

It could also be proved that the simulations can be used for all rotor sizes between  $D=0.25\text{m}$  and  $D=1.0\text{m}$ .

For a realtime estimation of the wake deflection (e.g. flight simulation or realtime aircraft formation during measurement campaigns) the extensive actuator disc parameters studies can be used to set up a simplified analytical or numerical model with D.L., angle of attack and inflow speed as input parameters.

What has not been investigated yet is the behavior of several rotors in a multicopter configuration. It has been assumed that the rotors are far enough apart so that no difference to an isolated rotor

occurs. This could be investigated by further simulations.

For the real measurement campaign an inflight validation of the measurement system is mandatory. This could be for example a comparison with a met mast. A comparison between running rotors and stopped rotors will be difficult in a field experiment due to the varying inflow conditions.

## **11. ACKNOWLEDGEMENTS:**

The ANWIND project was founded by the German Federal Ministry for Economic Affairs and Energy (BMWi). This support is gratefully acknowledged. The authors also would like to thank the Institute of Aerodynamics and Gas Dynamics at the University of Stuttgart making the wind tunnel tests possible. We would like to thank in particular Mr. Bernd Peters for his great support and advice.

Furthermore we are grateful for the help in modeling the actuator disc with ANSYS CFX offered by Mr. Matthias Arnold.

## **12. REFERENCES**

- [1] G. Giebel (ed.), U.Schmidt Paulsen, J. Bange, A. la Cour-Harbo, J. Reuder, S. Mayer, A. van der Kroonenberg, J. Mølgaard, "Autonomous Aerial Sensors for Wind Power Meteorology - A Pre-Project", Risø-R-1798(EN) January 2012.
- [2] MASC - a small Remotely Piloted Aircraft (RPA) for wind energy research, Wildmann, N; Hofsäß, M; Weimer, F; Joos, A; Bange, J. Advances in Science and Research.
- [3] Aerodynamics of V/STOL Flight, Barnes W. McCormick Jr., Dover Publications Inc., 1967
- [4] Tidal Current Turbine Wake and Park Layout in transient Environments, Arnold M, Cheng, P.W., Daus, P, Biskup F., Proceedings of the ASME 2014 33rd International Conference on Ocean, Offshore and Arctic Engineering, OMAE2014, June 8-13, 2014, San Francisco, California, USA